HIGH-FIDELITY MODELLING OF DAMAGE MECHANISMS IN THROUGH-THICKNESS REINFORCED COMPOSITES

António R. Melro[1], Hao Cui[2], Nik Petrinic[2], Ivana K. Partridge[1] and Stephen R. Hallett[1]

[1] Advanced Composites Collaboration for Innovation and Science
University of Bristol, Queen's Building, University Walk, Bristol BS8 1TR, United Kingdom
antonio.melro@bristol.ac.uk

[2] Department of Engineering Science, University of Oxford, Oxford, United Kingdom

Keywords: Through-thickness reinforcement, Finite element analysis, Damage tolerance

ABSTRACT

A high-fidelity model of a composite through-thickness reinforced with a z-pin was generated in order to study and characterise the increase in damage tolerance brought by this type of reinforcement. A coupled cohesive-friction interface model was developed and implemented to characterise the frictional behaviour between the z-pin's surface and the composite during the different stages of damage propagation. A thermo-visco-plastic constitutive model is used to model the epoxy behaviour. Failure of the z-pin is captured considering a maximum tensile failure and maximum longitudinal shear failure criteria. High-fidelity of the geometry of the model is achieved thanks to an automated script capable of reproducing all geometrical features of the reinforcement. Different mixed mode loading conditions (tension and/or shear) were applied to the model and the apparent increase in toughness, as well as the different phenomena leading to this increase were captured. The study was repeated for different stacking sequences next to the delamination plane so that a more reliable design of experiments could be performed, especially in a high-rate testing regime.

1 INTRODUCTION

High velocity impact threats set a requirement for controlling the propagation of delamination damage in the design and certification of structural components made from fibre reinforced composites [1]. By themselves, composite materials are not resistant to delamination onset and propagation. To address this issue, through-thickness reinforcements are inserted in the composite providing an apparent increase in the interfacial fracture toughness and improving their delamination tolerance [2].

One of the most used techniques for through-thickness reinforcement is z-pinning [3], whereby thin fibrous or metallic pins are inserted through the thickness of the laminate. The apparent increase in fracture toughness brought by this technique is dependent on a number of variables (geometry, loading, and material properties) of both z-pin and laminate.

Given the difficulty in exploring and/or controlling the effect of each of these variables in the performance of z-pinned composites through experimentation, the development of a high-fidelity numerical model to investigate the influence of such parameters provides the necessary insight into the different damage mechanisms occurring in the specimen.

Most of the numerical work available in the literature so far is dedicated to modelling mode I interlaminar delamination of z-pinned composites. One of the early attempts was conducted by Grassi et al. [4-5] where an analytical micro-mechanical model of the z-pin pull-out process was deduced to characterise mode I delamination. Dantuluri et al. [6] defined a quadri-linear cohesive zone law to characterise mode I delamination of a z-pinned composite in a DCB test.

Bianchi et al. [7] created a single-pin model considering axi-symmetric geometry, and have modelled the pull-out force as a function of displacement using a tri-linear or a bi-linear cohesive law, for low and high friction resistance, respectively, at the pin-laminate interface. The results were then used as calibration for modelling a DCB test of a z-pinned composite. Bianchi et al. have then applied this approach to characterise mode II behaviour [8].

Cui et al. [9] performed micromechanical analyses trying to capture the different bridging mechanisms in z-pins. A simplified 2D model was generated using plane stress elements, and layers of cohesive elements were positioned to capture splitting and tensile failure of the pin. The interface between the z-pin and the laminate was modelled using a combination of cohesive and frictional laws. The novelty on this approach was the application of a single model to different loading conditions. As a result, bridging maps were generated, accounting for different loading mode ratios (mode I, mode II, and mixed-mode).

Zhang et al. [10] extended the micromechanical approach into a full 3D model, accounting for pin misalignment, fibre waviness, failure of pin in tension and shear, mixed-mode loading, thermal and mechanical loading. Up to date, this was the most detailed numerical model ever developed.

This paper presents an extended version of the numerical model developed by Zhang et al. [10] with several updates to the constitutive material laws, contact interaction between pin and laminate, and geometry model generation.

2 MODEL DESCRIPTION

A Matlab® script has been written to generate the high-fidelity finite element models. This script allows the user to control a series of input parameters such as the geometry and area of influence of the z-pin, misalignment of z-pin, generated mesh density, stacking sequence of the laminate and material orientation to account for fibre waviness, location of a pre-existing delamination plane (if required), and mixed mode loading. The script also allows for the definition of all the contact areas in the model. The generated model can then be exported to either Abaqus® or LS-DYNA®.

Fig. 1 demonstrates an example of a generated model for a 16-layered laminate, with the stacking sequence $[(0,45,90,-45)_S, (90,-45,0,45)_S]$. On the left side of Fig. 1 a cut view of the pinned laminate is shown, providing insight on the different orientations of each layer as can be seen from the different cut angles on each pocket of resin. Also visible is the misalignment of the z-pin relative to the laminate.

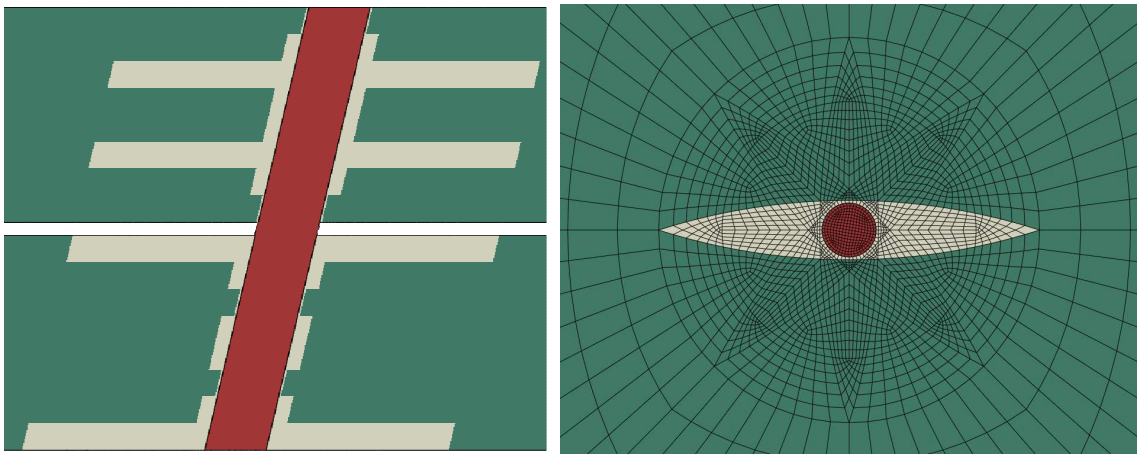

Figure 1: Example of generated model of z-pinned laminate. Elements in green represent laminate, white for the epoxy pocket around the z-pin and red for the z-pin (left: cut view; right: top view).

The script also allows the user to specify if longitudinal splitting of the z-pin should be modelled or not. This option is required since there are different materials from which a z-pin can be manufactured (metallic and fibrous) and not all are prone to this damage mechanism.

3 CONSTITUTIVE MODELLING

This section elaborates on the constitutive models used for the numerical analyses. Only continuum solid elements with 8 nodes and reduced order integration are used (element C3D8R from Abaqus® element library).

3.1 Laminate

The laminate is modelled considering the local increase in fibre volume fraction caused by insertion of the pin. This effect has been measured using high-resolution images of a cross-section and analysing fibre distribution in the vicinity and away from the z-pin. A local maximum of fibre volume fraction in the laminate has been found to exist close to the z-pin of up to 75%, compared to normal values away from the z-pin of around 60%.

This variation has been modelled using an analytical micromechanical model by Mori-Tanaka [11] which provides an estimate of the elastic properties of the composite as a function of the volume fraction and individual properties of each constituent – fibre and matrix.

Fig. 2 shows the distribution of fibre volume fraction in the laminate around the z-pin. For each integration point, a different value of volume fraction exists which will correspond, after application of Mori-Tanaka's model, to different elastic properties at each integration point. Along with elastic properties, also material orientation is slightly rotated at each integration point to consider the fibre misalignment as a z-pin is inserted in the laminate (Fig. 3).

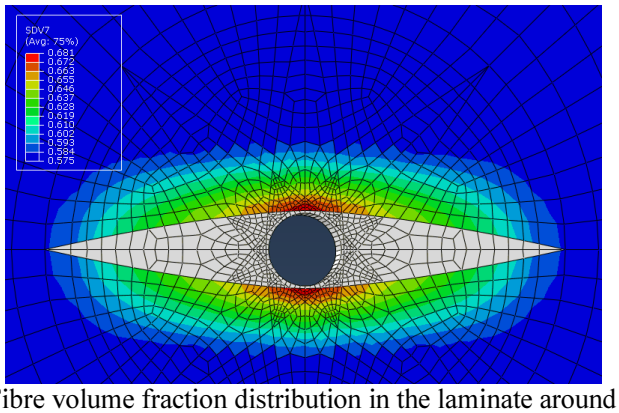

Figure 2: Fibre volume fraction distribution in the laminate around the z-pin.

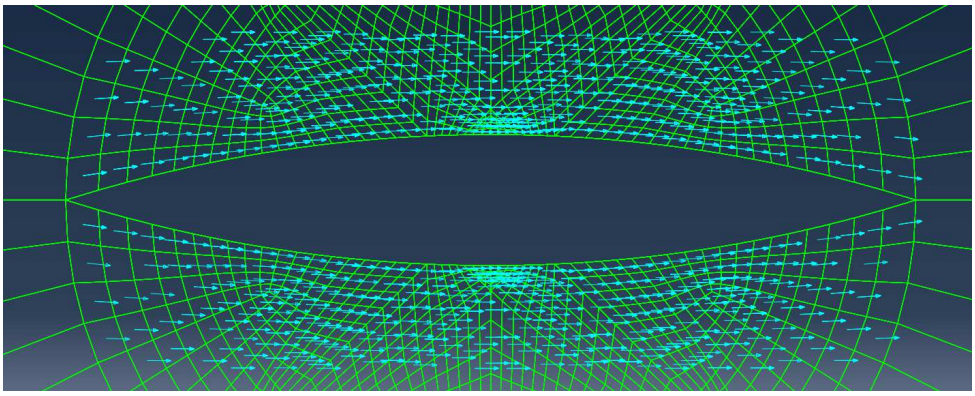

Figure 3: Fibre direction in the laminate around the z-pin.

3.2 Epoxy pocket

When a z-pin is inserted, fibres in the laminate are pushed aside and a resin-rich region is formed around the z-pin. This region is represented in white in Fig. 1. The resin is modelled with an elasto-plastic with damage constitutive model recently proposed to model the behaviour of epoxy resins [12].

The model follows a paraboloidal yield criterion which accounts for the pressure sensitivity of traditional epoxies. Isotropic damage uncoupled from the plastic model is considered. Further developments of this model [13] can capture the strain-rate and temperature dependencies of epoxies.

3.3 Z-pin

The z-pin is modelled with a linear elastic transverse isotropic law. Two damage mechanisms are considered: longitudinal tension and longitudinal shear.

In order to avoid symmetry problems and the appearance of mirror fracture planes in tension, each element is assigned with a slightly different value of tensile strength. The variation of strength can be observed in Fig. 4, where elements in blue have lower strength, while elements in red represent stronger material. The tensile strength is assigned at each element following a random distribution of values around the strength at the element obtained after application of a strength scaling criterion based on Weibull's criterion.

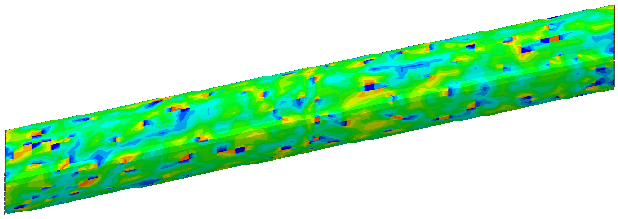

Figure 4: Strength distribution along the z-pin.

Splitting of the pin is modelled by considering thin solid elements along the axis of the z-pin. Only these elements are allowed to fail in both longitudinal tension and shear. Failure in shear is activated by a maximum shear stress criterion. The splitting elements are located along the pin and aligned with the direction of maximum shear stress under bending.

3.4 Interface z-pin/Laminate

The interface between the z-pin and the laminate is modelled through a user defined interfacial constitutive behaviour in Abaqus® using the general contact algorithm. The formulation is implemented through a VUINTERACTION subroutine. The contact model follows the approach introduced by Alfano and Sacco [14] which combines a bi-linear cohesive formulation with Mohr-Coulomb's frictional model. Differently from the original contribution by Alfano and Sacco [14], the cohesive formulation used for the current model was based on Jiang et al. [15]. Coupling with the frictional model is achieved by decomposing the contact domain associated with each contact point into a damaged and an undamaged contact area. The traction defined by the cohesive law is given by:

$$\mathbf{t} = (1 - d)K\boldsymbol{\delta} \tag{1}$$

where d represents the percentage of damaged area, K is the elastic stiffness and $\boldsymbol{\delta}$ the displacement vector. Friction can be active in the damaged contact area in a proportional way to the damage variable:

$$\mathbf{t} = (1 - d)\mathbf{t}^{\mathbf{u}} + d\mathbf{t}^{\mathbf{d}} \tag{2}$$

In equation (2), $\mathbf{t}^{\mathbf{u}}$ represents the traction vector in the undamaged contact area, and $\mathbf{t}^{\mathbf{d}}$ is the traction vector in the damaged contact area. This last vector is defined in a similar approach to a yield

criterion. The total displacement vector **δ** is decomposed in an elastic and a 'plastic' or permanent displacement $\boldsymbol{\delta}^{\mathbf{p}}$.

$$\mathbf{t}^{\mathbf{d}} = K\left(\delta - \delta^{p}\right) \tag{3}$$

The 'yield' function Φ, which in this case represents friction, is introduced such that Φ<0 corresponds to elastic behaviour ($\boldsymbol{\delta}^{\mathbf{p}}$=0), Φ=0 corresponds permanent displacement, and Φ>0 is impossible. The friction function Φ is defined by:

$$\Phi\left(\mathbf{t}^{\mathbf{c}}\right) = \mu\sigma^{d} + \left|\tau^{d}\right| - \tau_{0} \tag{4}$$

where μ is the friction coefficient, σ^d and τ^d are the normal and shear components of interfacial stress, and τ_0 represents a residual shear stress existing in the interface after complete failure and representing the roughness of the fracture surface.

The permanent displacement is defined by:

$$\delta^{p} = \lambda\begin{Bmatrix} 0 \\ \tau^{d} \Big/ \left|\tau^{d}\right| \end{Bmatrix} \tag{5}$$

where λ is a multiplier defined according to the Kuhn-Tucker conditions:

$$\lambda \geq 0, \quad \Phi\left(\mathbf{t}^{\mathbf{d}}\right) \leq 0, \quad \lambda \cdot \Phi\left(\mathbf{t}^{\mathbf{d}}\right) = 0 \tag{6}$$

The advantage of coupling a dry frictional model to a cohesive formulation is that once damage is complete and the cohesive bonding is no longer active, there is still the possibility for energy dissipation due to friction between the surfaces in contact. Also, this implementation guarantees the increase in both shear strength and toughness in the presence of a compressive stress, as observed by Li et al. [16], and demonstrated in Fig. 5.

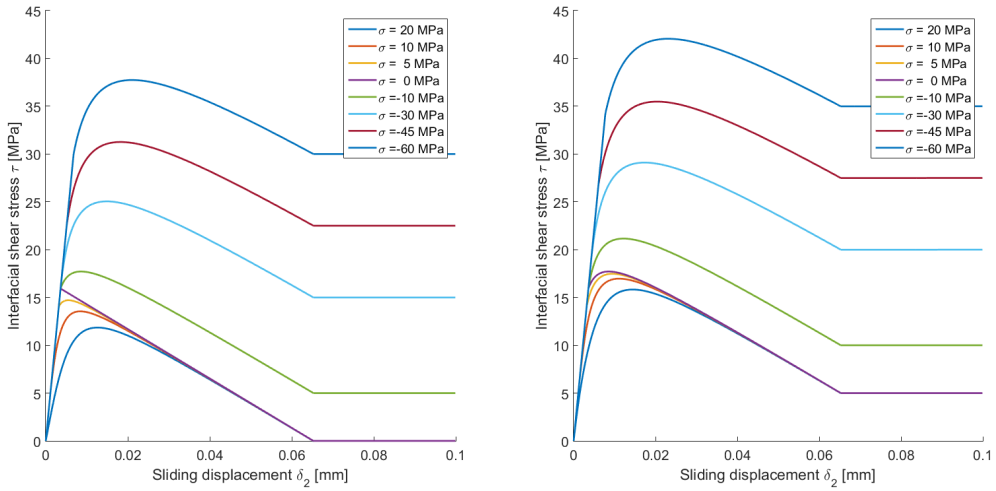

Figure 5: Interfacial shear stress under a constant normal tension or compression. a) without residual shear stress (τ_0 = 0); b) with residual shear stress (τ_0 = 5 MPa).

In Figure 5, the influence of a tensile or compressive stress is shown on the interfacial shear stress. With increasing compressive force, there is an increase in both shear strength and toughness. The effect of a residual shear stress (τ_0) is also noticeable in Figure 5b); this variable accounts for the shear stress existent in the pin surface due to the roughness of the damaged surface. Without this contribution, a perfectly aligned pin under a perfect pull-out load would slide out of the laminate without offering any resistance to the pull-out load.

4 FINITE ELEMENT ANALYSES

The capabilities of this high-fidelity modelling approach are evidenced by capturing the structural response of a z-pin when under different loading conditions along the delamination plane. The main objective of this model is to quantify the bridging force and the apparent increase in toughness, accorded by the presence of z-pins in laminates. For that, the finite element (FE) model is generated with an already existing delamination plane. Therefore, the obtained bridging force from these analyses will be that contributed by the z-pin alone.

Different mixed-mode quasi-static loadings are applied. Pin misalignment is incorporated in the geometry of the FE model (vide Fig. 1). Results of the FE analyses are compared with previously acquired experimental data [17]. Material properties used in the analyses are summarised in Table 1.

Fibre		Epoxy		Z-pin		Interface z-pin/laminate	
E_1 [MPa]	225000	E [MPa]	4600	E_1 [MPa]	144000	K_I [N/mm]	117600
E_2 [MPa]	15000	ν	0.35	E_2 [MPa]	7310	K_2 [N/mm]	44200
ν_{12}	0.2	α [°C $^{-1}$]	58e-6	ν_{12}	0.25	σ_{max} [MPa]	10.6
G_{12} [MPa]	15000	ν_P	0.3	G_{12} [MPa]	4450	τ_{max} [MPa]	15.9
G_{23} [MPa]	7000	X_t [MPa]	65	G_{23} [MPa]	2630	G_{cI} [N.mm]	0.16
α_{11} [°C $^{-1}$]	-0.5e-6	X_c [MPa]	180	α_{11} [°C $^{-1}$]	0	G_{cII} [N.mm]	0.52
α_{22} [°C $^{-1}$]	15e-6	G_{cI} [N.mm]	0.09	α_{22} [°C $^{-1}$]	30e-6	τ_0 [MPa]	10.0
				X_t [MPa]	1860	μ	0.3-0.9
				S_L [MPa]	120		
				G_{cI} [N.mm]	1.0		
				G_{cII} [N.mm]	1.0		
				Weibull parameter	35		

Table 1: Material properties.

The material properties for the interface z-pin/laminate were obtained from a mode I pull-out test case on a fully embedded single pin with 2 mm of length [17]. The only parameter that cannot be experimentally obtained is the friction coefficient μ for the interface pin/laminate. A parametric study was conducted to determine the correct value for the friction coefficient. Three values were assigned for μ: 0.3, 0.6, 0.9. Fig. 6 presents the results of this parametric study, where the value of μ = 0.6 was identified as the most suitable for the forthcoming analyses.

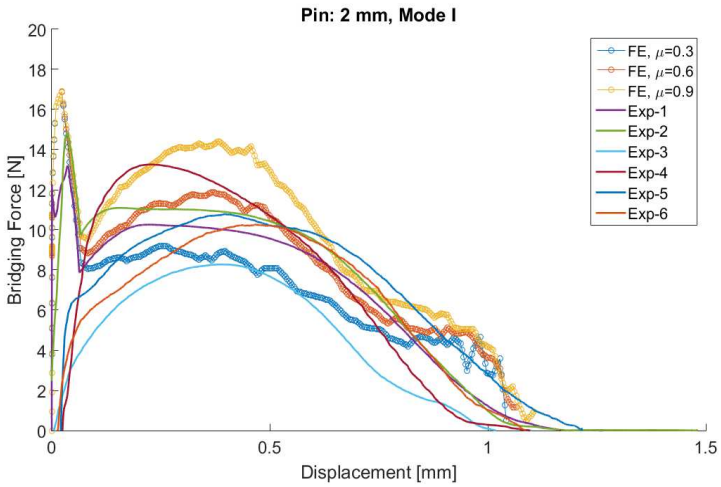

Figure 6: Results from parametric study to identify friction coefficient between z-pin and laminate.

A different loading direction has been applied to the same z-pin, and using the same material properties as per Table 1. For a pure mode II loading case, results are presented in Fig. 7. For demonstrative purposes, a mixed-mode loading case at 30° (shear dominated) is also presented in Fig. 8.

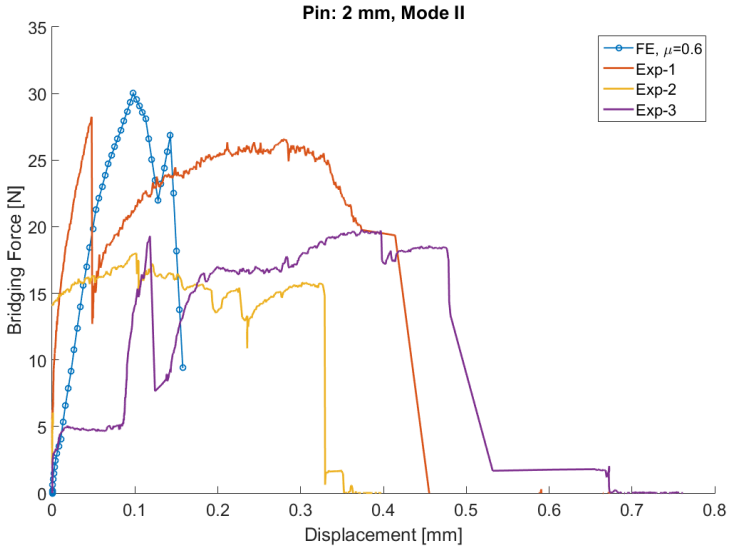

Figure 7: Results for a 2 mm long z-pin under a pure mode II loading condition.

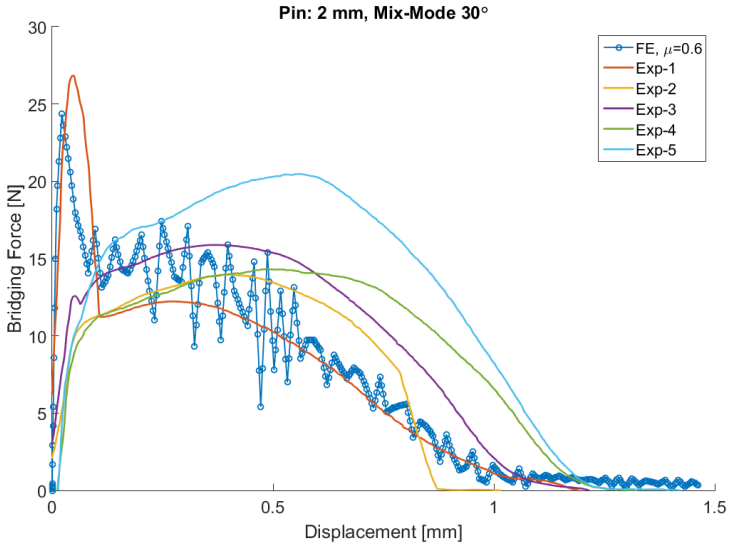

Figure 8: Results for a 2 mm long z-pin under a mix-mode at 30° (tension dominated) loading condition.

The model is able to capture most of the relevant features of the experimental data, although it still requires further validation against different lengths of z-pins. The influence of the number of splitting planes in the final bridging force is also under examination.

A common simplification is considering a perfectly aligned pin and a misaligned load instead of considering the real misalignment angle of the pin in the geometry of the model and a perfectly aligned load. Using this model, it was possible to demonstrate that there is no considerable difference at a macro-scale, as shown in Fig. 9. The bridging force follows a very similar pattern independently of the geometry. However, the model appears more stable if the real geometry is used.

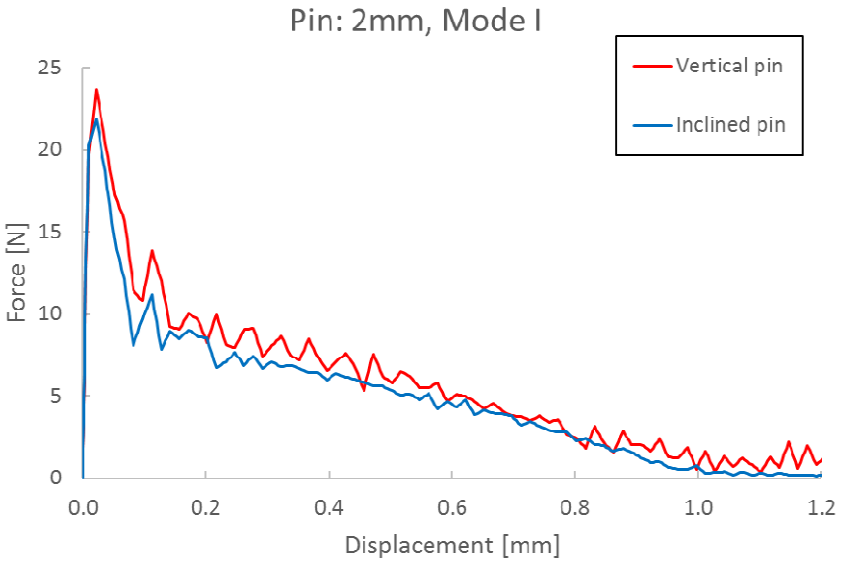

Figure 9: Comparison between a vertical z-pin and a real-misaligned z-pin.

There is however a difference at a micro-scale between the two approaches. When the real geometry of the z-pin is used, damage by longitudinal shear is activated in less splitting planes, which contributes to the overall steadier behaviour of the analysis. Also, the epoxy pocket in the first layers next to the delamination plane will be under a different triaxial state, mostly due to compression from the z-pin's contact pressure in the real-misaligned geometry. This will lead to a faster hardening of the epoxy material in that local region, but with very little influence in the macro-scale behaviour.

5 CONCLUSIONS

High-fidelity finite element (FE) models of through-thickness reinforced laminates using z-pins have been developed. An automated script can generate the FE models quickly, while still providing the user with a great level of control over the geometry, loading conditions, mesh size and stacking sequence of the laminate.

The constitutive behaviour of the laminate, z-pin, epoxy and interface between z-pin and laminate have been carefully addressed in order to capture the individual behaviour of each component and their contribution to the overall bridging force accorded by the presence of the z-pin.

Experimental data was used to obtain the mechanical properties of the interface between z-pin and laminate. Numerical predictions of the bridging force are shown to correlate well with the available experimental data, although further validation is required, namely with regards to different lengths of z-pin. Such detailed understanding from the models is necessary as one moves into the dynamic loading regime, where experimental data are much more difficult to interrogate and the fidelity of information gained, especially during the testing, is limited.

REFERENCES

[1] S. Georgiadis, A.J. Gunnion, R.S. Thomson, B.K. Cartwright, Bird-strike simulation for certification of the Boeing 787 composite moveable trailing edge, *Composites Structures*, **86**, 2009, pp. 258-268 (doi: 10.1016/j.compstruct.2008.03.025).

[2] A.P. Mouritz, Review of z-pinned composite laminates, *Composites Part A Applied Science and Manufacturing*, **38**, 2007, pp. 2383-2397 (doi: 10.1016/j.compositesa.2007.08.016).

[3] D.D.R. Cartié, I.K. Partridge, *Delamination behaviour of z-pinned laminates*, ESIS Publications, Vol. 27, Elsevier, 2000.

[4] M. Grassi, X. Zhang, Finite element analyses of mode I interlaminar delamination in z-fibre reinforced composite laminates, *Composites Science and Technology*, **63**, 2003, pp. 1815-1832 (doi:10.1016/S0266-3538(03)00134-9).

[5] M. Meo, F. Achard, M. Grassi. Finite element modelling of bridging micro-mechanics in through-thickness reinforced composite laminates, *Composite Structures*, **71**, 2005, pp. 383-387 (doi: 10.1016/j.compstruct.2005.09.025).

[6] V. Dantuluri, S. Maiti, P.H. Geubelle, R. Patel, H. Kilic. Cohesive modelling of delamination in z-pin reinforced composite laminates, *Composites Science and Technology*, **67**, 2007, pp. 616-631 (doi: 10.1016/j.compscitech.2006.07.024).

[7] F. Bianchi, X. Zhang. A cohesive zone model for predicting delamination suppression in z-pinned laminates, *Composites Science and Technology*, **71,** 2011, pp. 1898-1907 (doi: 10.1016/j.compscitech.2011.09.004).

[8] F. Bianchi, X. Zhang. Predicting mode-II delamination suppression in z-pinned laminates, *Composites Science and Technology,* **72**, 2012, pp. 924-932 (doi: 10.1016/j.compscitech.2012.03.003).

[9] H. Cui, Y. Li, S. Koussios, L. Zu, A. Beukers, Bridging micromechanisms of z-pin in mixed mode delamination, *Composite Structures,* **93**, 2011, pp. 2685-2695 (doi: 10.1013/j.compstruct.2011.06.004).

[10] B. Zhang, G. Allegri, M. Yasaee, S.R. Hallett, Micro-mechanical finite element analysis of Z-pins under mixed-mode loading, *Composites: Part A*, **78**, 2015, pp. 424-435 (doi: 10.1016/j.compositesa.2015.07.006).

[11] T. Mori, K. Tanaka, Average stress in matrix and average elastic energy of materials with misfitting inclusions, *Acta Metallurgica*, **21**, 1973, pp. 571-574 (doi: 10.1016/0001-6160(73)90064-3).

[12] A.R. Melro, P.P. Camanho, F.M.A. Pires, S.T. Pinho, Micromechanical analysis of polymer composites reinforced by unidirectional fibres: Part I – Constitutive modelling, *International Journal of Solids and Structures*, **50**, 2013, pp. 1897-1905 (doi: 10.1016/j.ijsolstr.2013.02.009).

[13] X. Bai, M.A. Bessa, A.R. Melro, P.P. Camanho, L. Guo, W.K. Liu, High-fidelity micro-scale modeling of the thermo-visco-plastic behavior of carbon fiber polymer matrix composites, *Composite Structures*, **134**, 2015, pp. 132-141 (doi: 10.1016/j.compstruct.2015.08.047).

[14] G. Alfano, E. Sacco, Combining interface damage and friction in a cohesive-zone model, *International Journal for Numerical Methods in Engineering*, **68**, 2006, pp. 542-582 (doi: 10.1002/nme.1728).

[15] W.G. Jiang, S.R. Hallett, B.G. Green, M.R. Wisnom, A concise interface constitutive law for analysis of delamination and splitting in composite materials and its application to scaled notched tensile specimens, *International Journal for Numerical Methods in Engineering*, **69**, 2007, pp. 1982-1995 (doi: 10.1002/nme.1842).

[16] X. Li, S.R. Hallett, M.R. Wisnom, Predicting the effect of through-thickness compressive stress on delamination using interface elements, *Composites: Part A*, **39**, 2008, pp. 218-230 (doi: 10.1016/j.compositesa.2007.11.005).

[17] M. Yasaee, L. Bigg, G. Mohamed, S.R. Hallett, Influence of z-pin embedded length on the interlaminar traction response of multi-directional composite laminates, *Materials and Design*, **115**, 2017, pp. 26-36 (doi: 10.1016/j.matdes.2016.11.025).